Nonvisual Arrestins Function as Simple Scaffolds Assembling the MKK4−JNK3α2 Signaling Complex

ARTICLE *in* BIOCHEMISTRY · NOVEMBER 2011

Impact Factor: 3.02 · DOI: 10.1021/bi201506g · Source: PubMed

4 AUTHORS, INCLUDING:

Xuanzhi Zhan
Vanderbilt University
13 PUBLICATIONS **186** CITATIONS
SEE PROFILE

Tamer Kaoud
University of Texas at Austin
48 PUBLICATIONS **314** CITATIONS
SEE PROFILE

Vsevolod V Gurevich
Vanderbilt University
195 PUBLICATIONS **12,017** CITATIONS
SEE PROFILE

Published in final edited form as:
Biochemistry. 2011 December 6; 50(48): 10520–10529. doi:10.1021/bi201506g.

Non-visual arrestins function as simple scaffolds assembling the MKK4–JNK3a2 signaling complex

Xuanzhi Zhan[1], **Tamer S. Kaoud**[2], **Kevin N. Dalby**[2], and **Vsevolod V. Gurevich**[1,*]

[1]Department of Pharmacology, Vanderbilt University, Nashville, TN 37232

[2]Division of Medicinal Chemistry, The University of Texas at Austin, Austin, TX 78712

Abstract

Arrestins are a small family of proteins with four mammalian members that play key roles in the regulation of multiple GPCR-dependent and -independent signaling pathways. Although arrestins were reported to serve as scaffolds for MAP kinase cascades, promoting the activation of JNK3, ERK1/2, and p38, the molecular mechanisms involved were not elucidated and even the direct binding of arrestins with MAP kinases were never demonstrated. Here using purified proteins we show that both non-visual arrestins directly bind JNK3α2 and its upstream activator MKK4, and that the affinity of arrestin-3 for these kinases is higher than that of arrestin-2. Reconstitution of the MKK4-JNK3α2 signaling module from pure proteins in the presence of different arrestin-3 concentrations showed that arrestin-3 acts as a “true” scaffold, facilitating JNK3α2 phosphorylation by bringing the two kinases together. Both JNK3α2 phosphorylation by MKK4 and JNK3α2 activity towards its substrate ATF2 increase at low and then decrease at high arrestin-3 levels, yielding bell-shaped concentration dependence expected with true scaffolds that do not activate the upstream kinase or its substrate. Thus, direct binding of both kinases and true scaffolding is the molecular mechanism of arrestin-3 action on the MKK4-JNK3α2 signaling module.

Keywords

arrestin; MAP kinase; scaffolding; JNK3; MKK4; affinity

Arrestins were first discovered as negative regulators of G protein-coupled receptor (GPCR) signaling (reviewed in (1, 2)). Arrestins bind to the cytoplasmic side of active receptors phosphorylated by GRKs, blocking further G protein coupling by steric exclusion (3, 4). Non-visual arrestin-2[1] and -3 facilitate GPCR recruitment to the coated pit by virtue of direct interactions of the arrestin C-tail with clathrin (5) and adaptor AP2 (6). Recent studies revealed a second, G protein-independent round of signaling inititated by the receptor-bound arrestins via interactions with a variety of non-receptor partners (reviewed in (7, 8)). In particular, the arrestin-receptor complex was reported to act as a scaffold for three mitogen-activated protein kinase (MAPK) cascades, leading to the activation of JNK3 (9), ERK1/2 (10), and p38 (11). While initial work suggested that only the arrestin-receptor complex

*Corresponding author: Vsevolod V. Gurevich, Department of Pharmacology, Vanderbilt University, Nashville, TN 37232; Tel.: 615-322-7070; vsevolod.gurevich@vanderbilt.edu.

Supporting Information Available. Supplemental Fig. S1 showing FRET between fluorescently labeled arrestin-2 and -3 and JNK3. This material is available free of charge via the Internet at http://pubs.acs.org.

[1]We use systematic names of arrestin proteins: arrestin-1 (historic names S-antigen, 48 kDa protein, visual or rod arrestin), arrestin-2 (b-arrestin or b-arrestin1), arrestin-3 (b-arrestin2 or hTHY-ARRX), and arrestin-4 (cone or X-arrestin; for unclear reasons its gene is called “*arrestin 3*” in HUGO database).

serves as the initiator of signaling (9–11), subsequent studies demonstrated that free arrestins interact with many of the same proteins (12–18) and appear to promote JNK3α2 activation independently of GPCRs (15, 18, 19).

MAPKs regulate critical cellular signaling pathways involved in cell proliferation, motility, differentiation and apoptosis (20). The core of all MAPK signaling modules conserved throughout eukaryotes comprises the three-kinase cascade, where MAP kinase kinase kinase (MAP3K) activates by phosphorylation MAP kinase kinase (MAP2K), whereupon it phosphorylates MAPK, which then phosphorylates different substrates (21, 22). Signal transduction in MAPK cascades is usually regulated by scaffolding proteins that assemble these kinases into signaling complexes. By tethering the kinase components into a multi-enzyme complex, the scaffolds provide an insulated physical conduit through which signals can be amplified and transmitted to the appropriate spatiotemporal cellular loci. Despite identification of new scaffold proteins and probing their functional roles, the molecular mechanisms of scaffolding remain unclear.

Using purified arrestin-2, arrestin-3, JNK3α2, and upstream MAP2K MKK4 here we demonstrated for the first time the direct interaction of JNK3α2 and MKK4 with both non-visual arrestins. By reconstruction of the arrestin-MKK4-JNK3α2 signaling module *in vitro* we show that arrestins act as true scaffolds, bringing JNK3α2 and its activator MKK4 together. Consistent with true scaffolding, the dependence of the JNK3α2 activation by MKK4 on arrestin-3 concentration is biphasic: an increase at lower levels is followed by a decrease at high arrestin-3. Kinetic analysis of JNK3α2 phosphorylation by MKK4 in the presence of different arrestin-3 concentrations also shows that the time course of JNK3α2 activation is significantly affected by scaffold concentration. This is the first experimental evidence demonstrating these theoretically predicted phonomena (23, 24).

Methods

Materials

All restriction enzymes were from New England Biolabs. Other chemicals were from sources previously described (25, 26).

Protein purification

Wild-type (WT) and mutant arrestin-2 and arrestin-3 proteins were purified, as previously described (27, 28). Briefly, untagged bovine arrestins were expressed in *Escherichia coli* and purified by sequential Heparin-Sepharose and Q-Sepharose chromatography to >95% purity, as judged by Coomassie staining. Two versions of His-tagged JNK2α2 with the same activity were used. In one, human JNK3α2 cDNA was subcoloned into pTrc-His2 vector between Nco I and Bam HI sites, so that the His6-tag was added on the C-terminus. In the other, JNK2α2 was His-tagged at the N-terminus, and the tag was cleaved off after purification. *Escherichia coli* strain BL21 (DE3) was used for expression. The cells were grown in LB to A_{600} = 0.4–0.8, then induced with 0.1 mM isopropyl β-D-thiogalactoside at 22°C for 5–6 h. The cells from 6L of culture were pelleted by centrifugation, resuspended in buffer containing 10 mM imidazole, 100 mM NaCl, and 20 mM Tris-HCl, pH 7.5, and lysed by freezing and thawing in the presence of lysozyme (3 mg/L), followed by sonication (three times for 15 seconds). After centrifugation (9,000 rpm for 90 min, Sorvall SLA-3000 rotor), the supernatants were passed through 5 ml nickel-NTA (Qiagene) chromatographic column. The column was washed with 50 ml of buffer containing 50 mM imidazole, 100 mM NaCl, and 20 mM Tris-Cl, pH 7.5. The proteins were eluted with 50 ml of the same buffer containing 250 mM imidazole. After adjusting NaCl concentration to 500 mM, the eluate was loaded onto 15 ml phenyl-Sepharose column, and eluted with 300 ml gradient from 0 to

70% ethylene glycol. Fractions containing JNK3α2 (50~80 ml) were diluted 10-fold with 5 mM Tris-HCl, pH 7.5, and loaded onto 10 ml SP-Sepharose column. JNK3α2 was eluted with 300 ml gradient from 0–300 mM NaCl in 20 mM Tris-Cl, pH 7.5 buffer. Fractions containing JNK3α2 (>95% purity) were pooled, concentrated to ~1 mg/ml, and stored at −80 °C.

Construction of pGEX4T1-MKK4

A construct encoding full-length wild type human mitogen-activated protein kinase kinase 4 (MAP2K4) (GenBank accession number NM_003010) with an N-terminal cleavable GST–tag was created by PCR amplification of an MKK4 template by using the following oligonucleotides: forward (5'-CGT **GGA TCC** ATG GCG GCT CCG AGC CCG AGC GGC GGC - 3') (Bam HI site in bold) and reverse (5'-CCG **CTC GAG** TTA TCA ATC GAC ATA CAT GGG AGA GCT GGG AGT - 3') (Xho I site in bold). The PCR product was digested with Bam HI and Xho I then ligated into a Bam HI-Xho I digested pGEX-4T1 vector. After transformation of the ligation mixture into DH5α *E. coli* cells with the appropriate antibiotic, the correct construct was recovered using standard molecular biology procedures. The sequence was verified at the institute for Cell and Molecular Biology (ICMB) Sequencing Facility at the University of Texas.

Expression and purification of GST-MKK4

The pGEX4T1-MKK4 vector was transformed into BL21 (DE3) electro-competent cells. A single colony of freshly transformed cells was inoculated in a 30 mL culture of Luria Broth (LB) containing 50 μg/mL ampicillin then incubated with shaking overnight at 37ºC. The culture was diluted 100-fold into TB (Terrific Broth) media containing 50 μg/mL ampicillin, and incubated with shaking at 37ºC until the OD_{600} reached 0.6–0.7. GST-MKK4 expression was induced by 25–50 μM IPTG, and shaking continued at 25ºC for 20 hours. The cells were pelleted (8000 × g, 15 min), immediately frozen in liquid nitrogen and stored at −80 ºC. Frozen wet cells were resuspended in 150 mL of Buffer A (10 mM Na_2HPO_4, 1.8 mM KH_2PO_4, pH 7.3, 140 mM NaCl, 2.7 mM KCl, 0.1% 2-mercaptoethanol, 0.1 mM TPCK, 0.1 mM PMSF and 1 mM benzamidine) containing 0.2 mg/mL lysozyme, 1 mM $MgCl_2$, and 20% (*v/v*) glycerol. The mixture was incubated at 4ºC for 30 minutes, then Triton-100 was added to a final concentration of 1% (*v/v*) and the incubation at 4ºC was extended for another 30 minutes. The cell lysate was sonicated at 4ºC for 5–10 minutes (at 5 s pulses with 5 s intervals and careful monitoring of the temperature using a temperature probe). The lysate was then centrifuged for 30 minutes at 12,000 × g and the supernatant mixed with 10 mL of Glutathione Sepharose™ High Performance (Amersham Biosciences) equilibrated in Buffer A and shaken gently for 1.5 h at 4 ºC. The beads were washed with 150 mL of Buffer A. The GST-tagged proteins were eluted with 20 mL buffer B (50 mM Tris HCl, pH 7.5, containing 20 mM reduced glutathione, 0.1% 2-mercaptoethanol, 0.1 mM TPCK, 0.1 mM PMSF, 1 mM benzamidine and 20% (v/v) glycerol). The eluted protein was collected and dialyzed into buffer S (25 mM HEPES pH 7.5, 50 mM KCl, 0.1 mM EDTA, 0.1 mM EGTA, 2 mM DTT) containing 20% glycerol. The protein was measured using Bradford reagent. The estimated yield was around 20–30 mg of pure GST-MKK4 per 1 L of cells.

Activation of GST-MKK4

4 μM GST-MKK4, 2 μM GST-MEKK1c (C terminal 320 amino acids corresponding to the catalytic domain) were incubated at 30 °C for 60 min in the presence of 4 mM ATP in 10 mL of activation buffer C (25 mM Hepes pH 7.5, 20 mM MgCl2, 0.1 mM EDTA, 0.1 mM EGTA and 2 mM dithiothrietol) and re-purified using a gel filtration column (120 mL HiLoad 16/60 Superdex 200 prep grade column) that had been equilibrated with 25 mM HEPES buffer (pH 7.5) containing 100 mM KCl, 0.1 mM EDTA, 0.1 mM EGTA and 2 mM

TCEP. This column purifies the active GST-MKK4 away from the constitutive active GST-MEKK1c. The activated GST-MKK4 was stored in buffer S containing 20% glycerol at −80 ºC until further use. At least 65% of GST-MKK4 was recovered as pure active GST-MKK4.

His-tag pull-down assay

Binding of arrestin-2 and -3 to His-tagged JNK3α2 was assayed by His-tag pull-down of the complex with Ni-NTA resin (Qiagen), according to the manufacturer's instructions. Briefly, 25 μl purified JNK3α2-His (20 mu;g) and 1 mM BSA were incubated with 25 mu;l Ni-NTA resin (50% slurry) in binding buffer (50 mM Hepes, pH 7.3, 150 mM NaCl) at 4°C with gentle rotation for 2 h. Subsequently, 50 mu;l of a solution containing 10 μg arrestin, 1 mM BSA, and 50 mM imidazole was added to a suspension of Ni-NTA-JNK3α2 and incubated at 4°C with gentle rotation for 2 h. The suspension were transferred to centrifuge filters (Ultrafree, Millipore) and washed three times with 200 mu;l wash buffer (50 mM imidazole, 50 mM Hepes, pH 7.3, 150 mM NaCl). The proteins were eluted from the Ni-NTA beads by the addition of 100 mu;l of elution buffer (250 mM imidazole, 50 mM Hepes, pH 7.3, 150 mM NaCl). The eluates were analyzed by SDS-PAGE and Western blot. Samples obtained in the absence of JNK3α2-His served as controls for non-specific binding.

GST pull-down assay

GST pull-down assay was used to analyze the binding of arrestin-2 and -3 to MKK4. 25 mu;l purified GST-MKK4 (10 mu;g) was incubated with 25 mu;l glutathione-agarose resin (50% slurry, Sigma) in binding buffer (50 mM Hepes, pH 7.3, 150 mM NaCl) at 4°C with gentle rotation for 2 h. 20 mu;l of arrestin (10 mu;g) was added, and the suspensions were incubated with rotation at 4°C for 2 h. The suspensions were transferred to centrifuge filters, and washed three times with 300 mu;l binding buffer. The proteins were eluted from resin by the addition of 100 mu;l of elution buffer (100 mM glutathione, 50 mM Hepes, pH 7.3, 150 mM NaCl). Eluates were analyzed by SDS-PAGE and Western blot. Samples obtained with GST bound to the column served as controls for non-specific binding.

Fluorescence Resonance Energy Transfer (FRET) assay

The binding affinities of both non-visual arrestins for MKK4 were determined using a FRET assay. Single cysteine mutants of arrestin-2 and -3 (arrestin-2-S234C, arrestin-3-L101C) genereated on the background of fully active cysteine-less mutants (25) were labeled with Fluorescein-5-Maleimide (Thermo Scientific), and wild-type JNK3α2 was labeled with Alexa Fluor 568 C_5 Maleimide (Invitrogen), according to the manufactures' protocols with minor modifications. The binding of proteins labeled with fluorescent probes was evaluated using a His-tag pull-down assay. FRET between donor fluorescein-labeled arrestins (50 nM) and acceptor Alexa 568-labeled JNK3 (0–10 mu;M) was measured in a spectrofluorometer (Photon Technology International). Fluorescence emission spectra were acquired at 25°C with excitation at 485 nm. Donor and acceptor only samples displayed distinct emission maxima at 518 and 600 nm, respectively (supplemental Fig. S1). The dissociation constants were calculated based on the decrease of the donor signal. The data were fitted to the one site binding equation using GraphPad Prism 4.

In vitro kinase activity assay: activation of JNK3α2 by MKK4

The effect of arrestins on the phosphorylation of JNK3α2 by MKK4 was analyzed by an *in vitro* MKK4 kinase activity assay. The assays were carried out in 10 mu;l containing the final concentrations of the following: 10 mM Hepes-Na, pH 7.3, 100 mM NaCl, 5 mM $MgCl_2$, 2 mM DTT, 50 nM active MKK4, 0.5 mu;M JNK3α2, and 0–30 mu;M arrestin-3. The reactions were initiated by the addition of 0.2 mM ATP (4 mu;Ci [γ-^{32}P]) and incubated individually at 30°C for the indicated time. The reactions were stopped by the addition of 15

mu;l Laemmli SDS sample buffer (Sigma), and subjected to PAGE (10%) electrophoresis. The gels were stained with Coomassie and dried. Phosphorylated JNK3α2 was visualized by autoradiography. The bands were cut out and the radioactivity was measured in a Tri-Carb Liquid Scintillation Counter (PerkinElmer).

Phosphorylation of ATF2 by JNK3α2

The enzymatic activity of JNK3α2 in the presence of MKK4 with or without arrestin-3 was determined by measuring the phosphorylation of the JNK3α2 substrate ATF2. The reactions were carried out in 10 mu;l containing 10 mM Hepes-Na, pH 7.3, 100 mM NaCl, 10 mM $MgCl_2$, 2 mM DTT, 50 nM active MKK4, 1 mu;M inactive JNK3α2, and 0–30 mu;M arrestin-3. The reactions were initiated by the addition of 0.3 mM ATP. After 4 minutes, 7 μl of the reaction mixture was transferred to another reaction mixture containing 20 mu;M purified GST-ATF2 (1–115) and 0.3 mM radiolabelled [γ-^{32}P]-ATP (specific activity = 1×10^{15} cpm/mol) in a final volume of 70 μl. The reaction mixture was incubated at 30°C. Aliquots (10 μL) were spotted onto P81 filter paper at different times (0.5, 1, 1.5, 2 and 4 min). The filter paper was washed three times for 15 minutes with 50 mM phosphoric acid to remove excess ATP, then once with acetone for drying. The amount of phosphate incorporated into ATF2 was determined by scintillation counting (Packard 1500).

RESULTS

MKK4 directly binds arrestin-2 and -3 with different affinity

Previous studies reported a weak association between MKK4 and arrestin-3, and this binding was enhanced in the presence of JNK3 and ASK1 (9). Recently we found that all four arrestins co-immunoprecipitate (co-IP) MKK4 (15). However, it remained unclear whether MKK4 binds arrestins directly or indirectly, as all previous studies used co-IP from cell lysates, where the interaction could have been mediated by any of the hundreds of other proteins present. To resolve this issue, we performed GST-pulldown to detect the binding between MKK4 with arrestin-2 and -3 using purified proteins (Fig. 1A), with equal amount of GST serving as a negative control (Fig. 1B). We found that MKK4 directly binds both non-visual arrestins. The binding to arrestin-3 was tighter than to arrestin-2, as judged by the presence of ~7.5 ± 2.4 ng of arrestin-3 and 0.8 ± 0.3 ng of arrestin-2 in 1/5 of the eluted sample (Fig. 1C). No non-specific binding to GST was detected. These data provide the first experimental evidence that MKK4 directly interacts with non-visual arrestins.

Higher binding to arrestin-3 than to arrestin-2 was a surprising finding, because co-IP studies suggested that both non-visual arrestins bind MKK4 similarly (15). However, the association of MKK4 with arrestins detected by co-IP was weak and may not have been sensitive enough to reveal different affinities of the two non-visual arrestins. The level of co-IP was also affected by the presence of the other kinases of this module, ASK1 and JNK3 (15). In contrast, the pull-down with purified proteins detects only the direct binding between arrestins and MKK4 in precisely controlled conditions, making this assay more reliable. Higher binding of arrestin-3 to MKK4 is consistent with an earlier demonstration that arrestin-3 is the only isoform that enhances JNK3α2 phosphorylation in COS-7 cells (9, 15, 19), although all arrestins bind all kinases in the ASK1-MKK4-JNK3 cascade (14, 15, 18, 29).

Arrestin-2 and -3 directly bind JNK3α2 with comparable affinity

The association with JNK3α2 was the first interaction between arrestins and MAP kinases described (9). The original study suggested that only arrestin-3 interacts with JNK3α2, and later a putative motif in the C-domain of arrestin-3, absent in arrestin-2, was tentatively identified as JNK3α2 binding site (19). This motif turned out to be specific for rodent

arrestin-3 (1), and subsequent studies showed that all arrestins interact with JNK3α2 and move it out of the nucleus to the cytoplasm (12–15, 29). JNK3α2 was also shown to bind comparably to WT arrestins, as well as "pre-activated" mutants and arrestins "frozen" in the basal conformation (14, 29). However, previous analysis of the interaction between JNK3 and arrestins was performed in cells, leaving open the possibility that this interaction is indirect, mediated by other cellular protein(s).

To investigate whether the binding between JNK3α2 and non-visual arrestins is direct, we used purified arrestins and JNK3α2-His in an *in vitro* His-tag pull-down assay (Fig. 2A, B, C). We found that both arrestin-2 and -3 directly associate with JNK3α2 and they bind it similarly (5.5 ± 0.9 ng arrestin-2 and 7.7 ± 1.2 ng arrestin-3 detected in 1/5 of eluted samples, respectively). These data are the first experimental demonstration that JNK3α2 directly binds non-visual arrestins. This finding raises the question of the affinity of these interactions. This information is critical to understand the biochemical mechanism of proposed arrestin-mediated scaffolding of MAPK cascades and to evaluate possible biological role of these processes in cells. We used FRET to determine the dissociation constants (K_D) between JNK3α2 and the two non-visual arrestins. Single cysteine mutants arrestin-2-L101C and arrestin-3-F234C were constructed on the background of fully functional cysteine-less arrestin-2 and –3 (17, 30) and labeled with fluoresceine (donor); wild type (WT) JNK3α2 was labeled with Alexa 568 (acceptor) at its natural solvent-exposed cysteines. His-tag pull-down was performed to compare the binding abilities of the unlabeled and fluorescently labeled proteins (Fig. 2C). The results showed that the addition of fluorescent probes does not significantly perturb arrestin interaction with JNK3α2 (Fig. 2C).

Upon excitation at 485 nm, donor-only samples (arrestin-2-L101F or arrestin-3-F234F, 50 nM) displayed a single fluorescence peak at 518 nm, while the acceptor-only samples (JNK3α2R, 1 mu;M) displayed only a fluorescence peak at 600 nm. Increased amplitude of the fluorescence peak at 600 nm was apparent in samples that contained both donor and acceptor (supplemental Fig. S1A, B). FRET was observed as both the decrease in the fluorescence of the arrestin-bound donor at 518 nm in the presence of the acceptor and an increase in fluorescence intensity of the acceptor at 600 nm. FRET titrations were performed by adding increasing concentrations of JNK3α2R, from 0.5 to 10 mu;M, to 50 nM fluoresceine-labeled arrestin (Fig. 2D, E). The dissociation constants were determined using the decrease of the donor signal upon the addition of the acceptor. JNK3α2R binds arrestin-2 and arrestin-3 with similar affinity, with K_D of 6.1±1.8 mu;M and 4.4±1.1 mu;M, respectively (Fig. 2F). These data represent the first direct measurement of the affinity of any arrestin for any MAP kinase.

Biphasic effect of arrestin concentration on JNK3α2 phosphorylation and activation by MKK4

Although proteins scaffolding MAP kinase cascades are believed to have profound effects on MAPK signaling, the biochemical mechanism of the function of scaffolds is poorly understood (31). Biphasic effect of scaffold concentration on MAPK signaling has been predicted by several computational models (23, 24, 31) and experimentally demonstrated only for Ste5, which scaffolds Ste4-Ste11-Ste7-Fus3 MAPK cascade in yeast *in vivo* (32). Figure 3A shows a simplified model illustrating Locasale's three-state mechanism (24) that explains the biphasic effect of the scaffold. According to this model, JNK3α2 can exist in three states: bound to upstream kinase MKK4 in solution, bound to scaffold protein not associated with MKK4 to form an incomplete complex, or bound to scaffold simultaneously with MKK4 in an active signaling complex. An increase of scaffold concentration in the lower range enhances the formation of an active complex containing both kinases, thereby facilitating the activation of the downstream kinase. In contrast, further increase of scaffold

concentration increases the probability of downstream and upstream kinase associating with the scaffold protein alone, forming incomplete inactive complexes. Therefore, the activation of MAPK by its upstream kinase can be inhibited by high concentration of scaffolds. Kinase suppressor of Ras (KSR), an ERK1/2 cascade scaffold protein, was the first mammalian MAPK scaffold shown to have a biphasic effect on the activation of ERK1/2 and its downstream signaling (33).

To directly test the mechanism of arrestin action, we used three purified proteins to reconstruct arrestin-3-MKK4-JNK3α2 signaling module. Since arrestin-3 was reported to be phosphorylated by another MAP kinase, ERK2 (34), we first tested whether active MKK4 and/or active JNK3α2 can phosphorylate non-visual arrestins (Fig. 3B). We found that neither active MKK4 nor active JNK3α2 phosphorylates arrestin-2 or arrestin-3 under our assay conditions. To evaluate the functional role of arrestins, we kept the concentrations of active MKK4 (50 nM) and its substrate unphosphorylated JNK3α2 (0.5 mu;M) constant, and measured JNK3α2 phosphorylation by MKK4 in the presence of various arrestin concentrations (0–30 mu;M). Both non-visual arrestins demonstrate bell-shaped concentration-dependence of JNK3α2 activation by MKK4. JNK3α2 phosphorylation was enhanced at low arrestin concentrations, but inhibited at higher concentrations. At 5 seconds, the highest level of JNK3α2 phosphorylation was observed in the presence of 0.6 mu;M arrestin-3. The optimal concentration of arrestin-3 at 10 seconds is higher, ~1.2 – 3 mu;M. Interestingly, arrestin-2 also promotes JNK3α2 phosphorylation by MKK4 in this *in vitro* assay, but demonstrates higher optimal concentrations at both time points (1.2 mu;M and 3–6 mu;M at 5 and 10 seconds, respectively) (Fig. 3C, D, E). Importantly, biphasic effect of arrestin concentrations was also observed by directly measuring the JNK3α2 activity. In these experiments purified active MKK4 was incubated with JNK3α2 in the presence or absence of arrestin-3, and then the ability of JNK3α2 to phosphorylate its substrate ATF2 was measured. From these data the apparent k_{cat} of JNK3α2 activated by MKK4 at various arrestin-3 concentrations was determined (Fig. 3G). These experiments yielded qualitatively similar results: JNK3α2 activation was facilitated by low, but inhibited at higher arrestin-3 concentrations, yielding bell-shaped concentration-dependence, with the highest JNK3α2 activity observed in the presence of 0.6 mu;M arrestin-3 (Fig. 3G), in excellent agreement with JNK3α2 phosphorylation data (Fig. 3F).

These findings are consistent with our direct binding data. The biphasic effect would only be observed when scaffolding protein binds both kinases (Fig. 3A). Higher optimal concentrations of arrestin-2 (Fig. 3E) are consistent with its significantly lower affinity for MKK4 (Fig. 1C). In addition to affinities of binary interactions, optimal scaffold concentrations can also be determined by positive or negative cooperativity of the simultaneous binding of the two kinases to the scaffolding protein (31). To further explore underlying mechanisms, we analyzed the time course of JNK3α2 activation at different arrestin-3 concentrations (0, 2 and 30 mu;M). In the presence of 2 μM arrestin-3, the initial rate of JNK3α2 activation by MKK4 (determined in the first 10 s) was increased from 12.63 ± 2.1 pmol/s to 19.2 ± 0.7 pmol/s; while at 30 μM arrestin-3 the initial rate was as low as in its absence, 10.7 ± 1.4 pmol/s.

DISCUSSION

Although arrestin-3-dependent JNK3α2 activation was reported more than a decade ago (9), direct interaction of any of the kinases in the ASK-MKK4-JNK3α2 cascade with arrestin-3 has never been demonstrated. In fact, the authors of the two initial studies hypothesized that ASK1 and JNK3α2 bind arrestin-3, whereas MKK4 does not (9, 19), and argued that arrestin-2 does not promote JNK3α2 activation because, in contrast to arrestin-3, it fails to bind this kinase (19). Subsequent work suggested that both non-visual arrestins comparably

bind JNK3α2 (13, 14, 18), MKK4 (15), and ASK1 (15), i.e., the binding per se does not account for the functional differences between arrestin-2 and –3 (15, 18). While the first report suggested that only receptor-associated arrestin-3 facilitates JNK3α2 phosphorylation (9), a subsequent study by the same group showed that free arrestin-3 can also accomplish this (19). The latter finding was confirmed using WT arrestin-3, as well as an arrestin-3 mutant impaired in receptor binding (15).

Arrestin-3 was termed a scaffold from the very beginning (9), even though all previous studies used exclusively cell-based assays and presented no evidence of direct interaction of any of the MAP kinases with arrestin-3 (12–15, 19, 29). Here we used purified proteins and several interaction assays to show for the first time that both JNK3α2 and MKK4 directly bind free arrestin-2 and arrestin-3 (Fig. 1B, C; Fig. 2). More than a hundred non-receptor partners were reported to bind arrestin-2 and –3 (35). However, very few of these interactions were shown to be direct, as co-IP, with or without subsequent proteomics analysis, used in most studies (9, 10, 15, 19, 35) shows that the proteins are in complexes that include arrestins, but cannot prove that any of them bind arrestins directly, rather than via another protein serving as an intermediary or scaffold. Considering recent keen interest in arrestin-mediated signaling (reviewed in (8, 36)), direct interaction with arrestins was demonstrated for surprisingly few non-receptor partners: clathrin (5, 37, 38), N-ethylmaleimide-sensitive fusion protein (39), PDE4D (40), microtubules (30, 41–43), calmodulin (16), MEK1 (44), and ubiquitin ligases AIP4 (45) and parkin (17). Various protein kinases were reported to interact with arrestins (reviewed in (7, 8)), but JNK3α2 and MKK4 are the first for which direct binding has been demonstrated (Fig. 1B, C; Fig. 2). We also measured the affinity of JNK3α2 interactions with non-visual arrestins (Fig. 2D, E, F). Taking into account typical rate constants for protein-protien interactions (46, 47), a K_D of 4–6 mu;M translates into a half-life of 0.12–0.17 seconds, which suggests that MAPK complexes with arrestins in cells are fairly transient, as could be expected to support rapid signaling events. Estimated arrestin-2 and -3 concentrations in neurons are sub-micromolar (48). Therefore, low micromolar affinity of JNK3α2 means that only a fraction of arrestins at any given moment exists in complex with this kinase in the cell. This is consistent with the notion that arrestins, which are too small to accommodate more than 3–4 proteins simultaneously (1), interact with multiple binding partners (7, 35), so that in the cell each partner associates with a small fraction of arrestins present. Interestingly, basal expression of Ste5 scaffold in yeast is much lower than necessary for maximum Fus3 activation, which likely allows for the regulation of signaling via changes of Ste5 expression in either direction (32). Similarly, the level of arrestin-3 in cells (48, 49) appears to be sub-optimal for the scaffolding of ASK1-MKK4-JNK3 cascade, possibly for the same reason.

Importantly, our experiments with the arrestin-3-MKK4-JNK3α2 complex reconstructed from purified proteins show that the ratio of the scaffold and the two kinases determines the time course of the signaling (Fig. 3). These data provide the first experimental support for the theoretical model proposed earlier (31). These results suggest that relatively low expression of arrestin-3 in mature neurons (48, 49) ensures rapid and transient JNK3α2 activation, which makes perfect biological sense in these irreplaceable post-mitotic cells. Arrestin-2 binds JNK3α2 and MKK4 (Fig. 2B; Fig. 1C), but does not activate JNK3α2 in cells (15, 19), suggesting that it acts in a dominant-negative fashion, suppressing JNK3α2 activity, thereby likely promoting cell survival. This is consistent with roughly equal expression of arrestin-2 and –3 in neuronal precursors (49), which is converted into a large 10–20-fold excess of arrestin-2 over arrestin-3 by means of rapid increase of arrestin-2 expression as neurons mature (48, 49).

While the idea that free arrestin-3 can promote JNK3α2 activation was proposed earlier (15, 19), our data provide the first unambiguous evidence that this is the case (Fig. 3).

Interestingly, our data suggest that quantitative differences in the affinity of arrestin-2 and –3 for these kinases translates into qualitative difference between lack of activity and effective JNK3α2 activation in the cell, where the levels of arrestins, MKK4, and JNK3α2 are relatively low and tightly regulated. Obviously, we cannot exclude the possibility that this difference is partially due to differential ASK1 binding, although indirect evidence based on co-IP suggests that this is unlikely (15, 18). This issue can be definitively resolved only by the reconstruction from pure proteins of complete ASK1-MKK-4-JNK3α2 signaling module with arrestin-2 and -3.

Arrestins in the cell exist in at least three distinct conformations: 1) free, closely resembling crystal structures (27, 50–53); 2) receptor-bound; and 3) microtubule-bound (reviewed in (54)). The proteins that engage well-defined receptor-binding surface (25, 55–60) do not interact with receptor-associated arrestins (16, 42, 61, 62). The partners whose interaction sites do not overlap with that of GPCRs show distinct conformational preferences: ERK2 appears to prefer receptor-bound arrestin (15, 26), ubiquitin ligases Mdm2 and parkin preferentially interact with arrestins in the basal conformation (14, 15, 17, 29), whereas JNK3α2 does not seem to care one way or the other (14, 15, 29). We demonstrated that free arrestin-3 at optimal concentration promotes JNK3α2 phosphorylation by MKK4. However, only direct kinetic comparison of this complex with the one similarly reconstructed from pure proteins containing receptor-associated arrestin-3 can definitively show whether receptor binding plays any role in this signaling other than simply concentrating the arrestins and associated kinases in the vicinity of receptor-rich membranes.

In conclusion, the first reconstruction from pure proteins of the signaling complex organized by arrestin revealed that both MKK4 and JNK3α2 directly bind free arrestin-3, which acts as a true scaffold facilitating JNK3α2 phosphorylation by MKK4 simply by simultaneously binding these two kinases, bringing them in close proximity. This work demonstrates that experiments with pure proteins in strictly controlled conditions can yield definitive answers that remained elusive when only cell-based assays were in use. Further experimentation with pure proteins is necessary to reveal possible differences in MAPK scaffolding by free and receptor-bound arrestins, which is necessary for the elucidation of the biological role of these events in cell signaling, as well as for devising ways of targeting this process for therapeutic purposes.

Supplementary Material

Refer to Web version on PubMed Central for supplementary material.

Acknowledgments

Funding: NIH grants GM077561, GM081756, EY011500 (VVG); GM059802 and Welch Foundation (F-1390) (KND).

Abbreviations

GPCR	G protein-coupled receptor
MAPK, or MAP kinase	mitogen-activated protein kinase
JNK3α2	c-Jun N-terminal kinase 3α2
MKK4	MAP kinase kinase4
ERK1/2	extracellular signal-regulated kinase1/2
GRK	G protein-coupled receptor kinase

GST	glutathione S-transferase
LB	Luria Broth
PMSF	phenylmethylsulfonylfluoride
FRET	fluorescence resonance energy transfer

References

1. Gurevich VV, Gurevich EV. The structural basis of arrestin-mediated regulation of G protein-coupled receptors. Pharm Ther. 2006; 110:465–502.
2. Gurevich VV, Hanson SM, Song X, Vishnivetskiy SA, Gurevich EV. The functional cycle of visual arrestins in photoreceptor cells. Prog Retin Eye Res. 2011; 30:405–430. [PubMed: 21824527]
3. Krupnick JG, Gurevich VV, Benovic JL. Mechanism of quenching of phototransduction. Binding competition between arrestin and transducin for phosphorhodopsin. J Biol Chem. 1997; 272:18125–18131. [PubMed: 9218446]
4. Wilden U. Duration and amplitude of the light-induced cGMP hydrolysis in vertebrate photoreceptors are regulated by multiple phosphorylation of rhodopsin and by arrestin binding. Biochemistry. 1995; 34:1446–1454. [PubMed: 7827093]
5. Goodman OB Jr, Krupnick JG, Santini F, Gurevich VV, Penn RB, Gagnon AW, Keen JH, Benovic JL. Beta-arrestin acts as a clathrin adaptor in endocytosis of the beta2-adrenergic receptor. Nature. 1996; 383:447–450. [PubMed: 8837779]
6. Laporte SA, Oakley RH, Zhang J, Holt JA, Ferguson sSG, Caron MG, Barak LS. The 2-adrenergic receptor/arrestin complex recruits the clathrin adaptor AP-2 during endocytosis. Proc Nat Acad Sci USA. 1999; 96:3712–3717. [PubMed: 10097102]
7. Gurevich EV, Gurevich VV. Arrestins are ubiquitous regulators of cellular signaling pathways. Genome Biology. 2006; 7:236. [PubMed: 17020596]
8. DeWire SM, Ahn S, Lefkowitz RJ, Shenoy SK. Beta-arrestins and cell signaling. Annu Rev Physiol. 2007; 69:483–510. [PubMed: 17305471]
9. McDonald PH, Chow CW, Miller WE, Laporte SA, Field ME, Lin FT, Davis RJ, Lefkowitz RJ. Beta-arrestin 2: a receptor-regulated MAPK scaffold for the activation of JNK3. Science. 2000; 290:1574–1577. [PubMed: 11090355]
10. Luttrell LM, Roudabush FL, Choy EW, Miller WE, Field ME, Pierce KL, Lefkowitz RJ. Activation and targeting of extracellular signal-regulated kinases by beta-arrestin scaffolds. Proc Natl Acad Sci U S A. 2001; 98:2449–2454. [PubMed: 11226259]
11. Bruchas MR, Macey TA, Lowe JD, Chavkin C. Kappa opioid receptor activation of p38 MAPK is GRK3- and arrestin-dependent in neurons and astrocytes. J Biol Chem. 2006; 281:18081–18089. [PubMed: 16648139]
12. Scott MG, Le Rouzic E, Perianin A, Pierotti V, Enslen H, Benichou S, Marullo S, Benmerah A. Differential nucleocytoplasmic shuttling of beta-arrestins. Characterization of a leucine-rich nuclear export signal in beta-arrestin2. J Biol Chem. 2002; 277:37693–37701. [PubMed: 12167659]
13. Wang P, Wu Y, Ge X, Ma L, Pei G. Subcellular localization of beta-arrestins is determined by their intact N domain and the nuclear export signal at the C terminus. J Biol Chem. 2003; 278:11648–11653. [PubMed: 12538596]
14. Song X, Raman D, Gurevich EV, Vishnivetskiy SA, Gurevich VV. Visual and both non-visual arrestins in their “inactive” conformation bind JNK3 and Mdm2 and relocalize them from the nucleus to the cytoplasm. J Biol Chem. 2006; 281:21491–21499. [PubMed: 16737965]
15. Song X, Coffa S, Fu H, Gurevich VV. How does arrestin assemble MAPKs into a signaling complex? J Biol Chem. 2009; 284:685–695. [PubMed: 19001375]
16. Wu N, Hanson SM, Francis DJ, Vishnivetskiy SA, Thibonnier M, Klug CS, Shoham M, Gurevich VV. Arrestin binding to calmodulin: a direct interaction between two ubiquitous signaling proteins. J Mol Biol. 2006; 364:955–963. [PubMed: 17054984]

17. Ahmed MR, Zhan X, Song X, Kook S, Gurevich VV, Gurevich EV. Ubiquitin ligase parkin promotes Mdm2-arrestin interaction but inhibits arrestin ubiquitination. Biochemistry. 2011; 50:3749–3763. [PubMed: 21466165]
18. Seo J, Tsakem EL, Breitman M, Gurevich VV. Identification of arrestin-3-specific residues necessary for JNK3 activation. J Biol Chem. 2011; 286:27894–27901. [PubMed: 21715332]
19. Miller WE, McDonald PH, Cai SF, Field ME, Davis RJ, Lefkowitz RJ. Identification of a motif in the carboxyl terminus of beta -arrestin2 responsible for activation of JNK3. Journal of Biological Chemistry. 2001; 276:27770–27777. [PubMed: 11356842]
20. Dhanasekaran DN, Kashef K, Lee CM, Xu H, Reddy EP. Scaffold proteins of MAP-kinase modules. Oncogene. 2007; 26:3185–3202. [PubMed: 17496915]
21. Yoshioka K. Scaffold Proteins in Mammalian MAP Kinase Cascades. Journal of Biochemistry. 2004; 135:657–661. [PubMed: 15213240]
22. Dard N, Peter M. Scaffold proteins in MAP kinase signaling: more than simple passive activating platforms. BioEssays. 2006; 28:146–156. [PubMed: 16435292]
23. Locasale JW, Chakraborty AK. Regulation of signal duration and the statistical dynamics of kinase activation by scaffold proteins. PLoS Comput Biol. 2008; 4:e1000099. [PubMed: 18584022]
24. Locasale JW. Three-state kinetic mechanism for scaffold-mediated signal transduction. Phys Rev E Stat Nonlin Soft Matter Phys. 2008; 78:051921. [PubMed: 19113169]
25. Vishnivetskiy SA, Gimenez LE, Francis DJ, Hanson SM, Hubbell WL, Klug CS, Gurevich VV. Few residues within an extensive binding interface drive receptor interaction and determine the specificity of arrestin proteins. J Biol Chem. 2011; 286:24288–24299. [PubMed: 21471193]
26. Coffa S, Breitman M, Spiller BW, Gurevich VV. A single mutation in arrestin-2 prevents ERK1/2 activation by reducing c-Raf1 binding. Biochemistry. 2011; 50:6951–6958. [PubMed: 21732673]
27. Zhan X, Gimenez LE, Gurevich VV, Spiller BW. Crystal structure of arrestin-3 reveals the basis of the difference in receptor binding between two non-visual arrestins. J Mol Biol. 2011; 406:467–478. [PubMed: 21215759]
28. Gurevich VV, Benovic JL. Arrestin: mutagenesis, expression, purification, and functional characterization. Methods Enzymol. 2000; 315:422–437. [PubMed: 10736718]
29. Song X, Gurevich EV, Gurevich VV. Cone arrestin binding to JNK3 and Mdm2: conformational preference and localization of interaction sites. J Neurochem. 2007; 103:1053–1062. [PubMed: 17680991]
30. Hanson SM, Cleghorn WM, Francis DJ, Vishnivetskiy SA, Raman D, Song X, Nair KS, Slepak VZ, Klug CS, Gurevich VV. Arrestin mobilizes signaling proteins to the cytoskeleton and redirects their activity. J Mol Biol. 2007; 368:375–387. [PubMed: 17359998]
31. Levchenko A, Bruck J, Sternberg PW. Scaffold proteins may biphasically affect the levels of mitogen-activated protein kinase signaling and reduce its threshold properties. Proc Natl Acad Sci U S A. 2000; 97:5818–5823. [PubMed: 10823939]
32. Chapman SA, Asthagiri AR. Quantitative effect of scaffold abundance on signal propagation. Mol Syst Biol. 2009; 5:313. [PubMed: 19888208]
33. Kortum RL, Lewis RE. The molecular scaffold KSR1 regulates the proliferative and oncogenic potential of cells. Mol Cell Biol. 2004; 24:4407–4416. [PubMed: 15121859]
34. Lin FT, Miller WE, Luttrell LM, Lefkowitz RJ. Feedback regulation of beta-arrestin1 function by extracellular signal-regulated kinases. J Biol Chem. 1999; 274:15971–15974. [PubMed: 10347142]
35. Xiao K, McClatchy DB, Shukla AK, Zhao Y, Chen M, Shenoy SK, Yates JR, Lefkowitz RJ. Functional specialization of beta-arrestin interactions revealed by proteomic analysis. Proc Natl Acad Sci U S A. 2007; 104:12011–12016. [PubMed: 17620599]
36. Gurevich VV, Gurevich EV. Custom-designed proteins as novel therapeutic tools? The case of arrestins. Expert Rev Mol Med. 2010; 12:e13. [PubMed: 20412604]
37. Krupnick JG, Goodman OB Jr, Keen JH, Benovic JL. Arrestin/clathrin interaction. Localization of the clathrin binding domain of nonvisual arrestins to the carboxy terminus. J Biol Chem. 1997; 272:15011–15016. [PubMed: 9169476]

38. Goodman OB Jr, Krupnick JG, Gurevich VV, Benovic JL, Keen JH. Arrestin/clathrin interaction. Localization of the arrestin binding locus to the clathrin terminal domain. J Biol Chem. 1997; 272:15017–15022. [PubMed: 9169477]
39. McDonald PH, Cote NL, Lin FT, Premont RT, Pitcher JA, Lefkowitz RJ. Identification of NSF as a beta-arrestin1-binding protein. Implications for beta2-adrenergic receptor regulation. J Biol Chem. 1999; 274:10677–10680. [PubMed: 10196135]
40. Baillie GS, Adams DR, Bhari N, Houslay TM, Vadrevu S, Meng D, Li X, Dunlop A, Milligan G, Bolger GB, Klussmann E, Houslay MD. Mapping binding sites for the PDE4D5 cAMP-specific phosphodiesterase to the N- and C-domains of beta-arrestin using spot-immobilized peptide arrays. Biochem J. 2007; 404:71–80. [PubMed: 17288540]
41. Nair KS, Hanson SM, Kennedy MJ, Hurley JB, Gurevich VV, Slepak VZ. Direct binding of visual arrestin to microtubules determines the differential subcellular localization of its splice variants in rod photoreceptors. J Biol Chem. 2004; 279:41240–41248. [PubMed: 15272005]
42. Nair KS, Hanson SM, Mendez A, Gurevich EV, Kennedy MJ, Shestopalov VI, Vishnivetskiy SA, Chen J, Hurley JB, Gurevich VV, Slepak VZ. Light-dependent redistribution of arrestin in vertebrate rods is an energy-independent process governed by protein-protein interactions. Neuron. 2005; 46:555–567. [PubMed: 15944125]
43. Hanson SM, Francis DJ, Vishnivetskiy SA, Klug CS, Gurevich VV. Visual arrestin binding to microtubules involves a distinct conformational change. J Biol Chem. 2006; 281:9765–9772. [PubMed: 16461350]
44. Meng D, Lynch MJ, Huston E, Beyermann M, Eichhorst J, Adams DR, Klusmann E, Houslay MD, Baillie GS. MEK1 binds directly to betaarrestin1, influencing both its phosphorylation by ERK and the timing of its isoprenaline-stimulated internalization. J Biol Chem. 2009; 284:11425–11435. [PubMed: 19153083]
45. Bhandari D, Trejo J, Benovic JL, Marchese A. Arrestin-2 interacts with the ubiquitin-protein isopeptide ligase atrophin-interacting protein 4 and mediates endosomal sorting of the chemokine receptor CXCR4. J Biol Chem. 2007; 282:36971–36979. [PubMed: 17947233]
46. Northrup SH, Erickson HP. Kinetics of protein-protein association explained by Brownian dynamics computer simulation. Proc Natl Acad Sci U S A. 1992; 89:3338–3342. [PubMed: 1565624]
47. Bayburt TH, Vishnivetskiy SA, McLean M, Morizumi T, Huang C-c, Tesmer JJ, Ernst OP, Sligar SG, Gurevich VV. Rhodopsin monomer is sufficient for normal rhodopsin kinase (GRK1) phosphorylation and arrestin-1 binding. J Biol Chem. 2011; 286:1420–1428. [PubMed: 20966068]
48. Gurevich EV, Benovic JL, Gurevich VV. Arrestin2 expression selectively increases during neural differentiation. J Neurochem. 2004; 91:1404–1416. [PubMed: 15584917]
49. Gurevich EV, Benovic JL, Gurevich VV. Arrestin2 and arrestin3 are differentially expressed in the rat brain during postnatal development. Neuroscience. 2002; 109:421–436. [PubMed: 11823056]
50. Hirsch JA, Schubert C, Gurevich VV, Sigler PB. The 2.8 A crystal structure of visual arrestin: a model for arrestin's regulation. Cell. 1999; 97:257–269. [PubMed: 10219246]
51. Han M, Gurevich VV, Vishnivetskiy SA, Sigler PB, Schubert C. Crystal structure of beta-arrestin at 1.9 A: possible mechanism of receptor binding and membrane translocation. Structure. 2001; 9:869–880. [PubMed: 11566136]
52. Milano SK, Pace HC, Kim YM, Brenner C, Benovic JL. Scaffolding functions of arrestin-2 revealed by crystal structure and mutagenesis. Biochemistry. 2002; 41:3321–3328. [PubMed: 11876640]
53. Sutton RB, Vishnivetskiy SA, Robert J, Hanson SM, Raman D, Knox BE, Kono M, Navarro J, Gurevich VV. Crystal Structure of Cone Arrestin at 2.3Å: Evolution of Receptor Specificity. J Mol Biol. 2005; 354:1069–1080. [PubMed: 16289201]
54. Gurevich VV, Gurevich EV, Cleghorn WM. Arrestins as multi-functional signaling adaptors. Handb Exp Pharmacol. 2008; 186:15–37. [PubMed: 18491047]
55. Ohguro H, Palczewski K, Walsh KA, Johnson RS. Topographic study of arrestin using differential chemical modifications and hydrogen/deuterium exchange. Protein Sci. 1994; 3:2428–2434. [PubMed: 7756996]

56. Pulvermuller A, Schroder K, Fischer T, Hofmann KP. Interactions of metarhodopsin II. Arrestin peptides compete with arrestin and transducin. J Biol Chem. 2000; 275:37679–37685. [PubMed: 10969086]
57. Gurevich VV, Benovic JL. Visual arrestin binding to rhodopsin: diverse functional roles of positively charged residues within the phosphorylation-recignition region of arrestin. J Biol Chem. 1995; 270:6010–6016. [PubMed: 7890732]
58. Vishnivetskiy SA, Hosey MM, Benovic JL, Gurevich VV. Mapping the arrestin-receptor interface: structural elements responsible for receptor specificity of arrestin proteins. J Biol Chem. 2004; 279:1262–1268. [PubMed: 14530255]
59. Hanson SM, Gurevich VV. The differential engagement of arrestin surface charges by the various functional forms of the receptor. J Biol Chem. 2006; 281:3458–3462. [PubMed: 16339758]
60. Hanson SM, Francis DJ, Vishnivetskiy SA, Kolobova EA, Hubbell WL, Klug CS, Gurevich VV. Differential interaction of spin-labeled arrestin with inactive and active phosphorhodopsin. Proc Natl Acad Sci U S A. 2006; 103:4900–4905. [PubMed: 16547131]
61. Hanson SM, Van Eps N, Francis DJ, Altenbach C, Vishnivetskiy SA, Arshavsky VY, Klug CS, Hubbell WL, Gurevich VV. Structure and function of the visual arrestin oligomer. EMBO J. 2007; 26:1726–1736. [PubMed: 17332750]
62. Hanson SM, Dawson ES, Francis DJ, Van Eps N, Klug CS, Hubbell WL, Meiler J, Gurevich VV. A model for the solution structure of the rod arrestin tetramer. Structure. 2008; 16:924–934. [PubMed: 18547524]

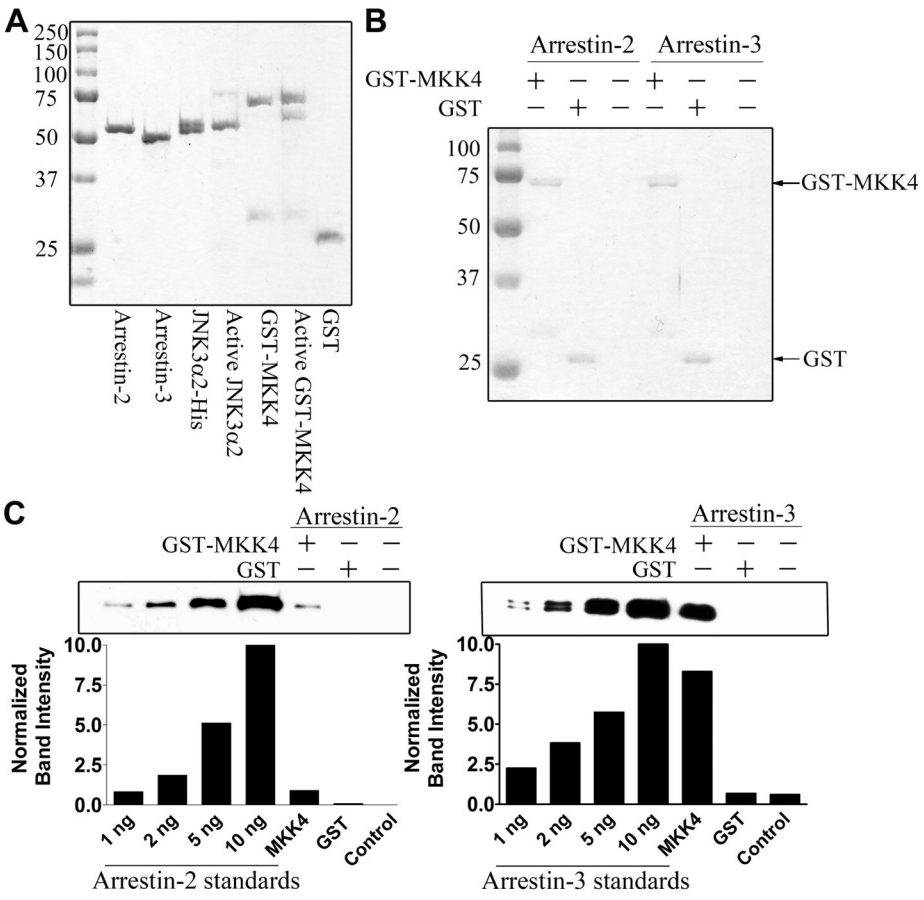

Fig. 1. Non-visual arrestins directly bind MKK4 with different affinities

A. Coomassie-stained SDS-PAGE gel showing the purity of indicated proteins used in this study. **B.** Coomassie staining of GST and GST-MKK4 eluted from glutathione column, showing equal loading. **C.** The results of GST pull-down showed that both non-visual arrestins are retained by GST-MKK4, but not by GST column. Western blots of the eluates from indicated columns (1/5 loaded); lanes containing known amounts of purified arrestin-2 and -3 were used as standards to generate calibration curves. Quantification shows that GST-MKK4 column retained 0.8 ± 0.3 and 7.5 ± 2.4 ng of arrestin-2 and –3, respectively. The results of a representative experiment out of three performed are shown.

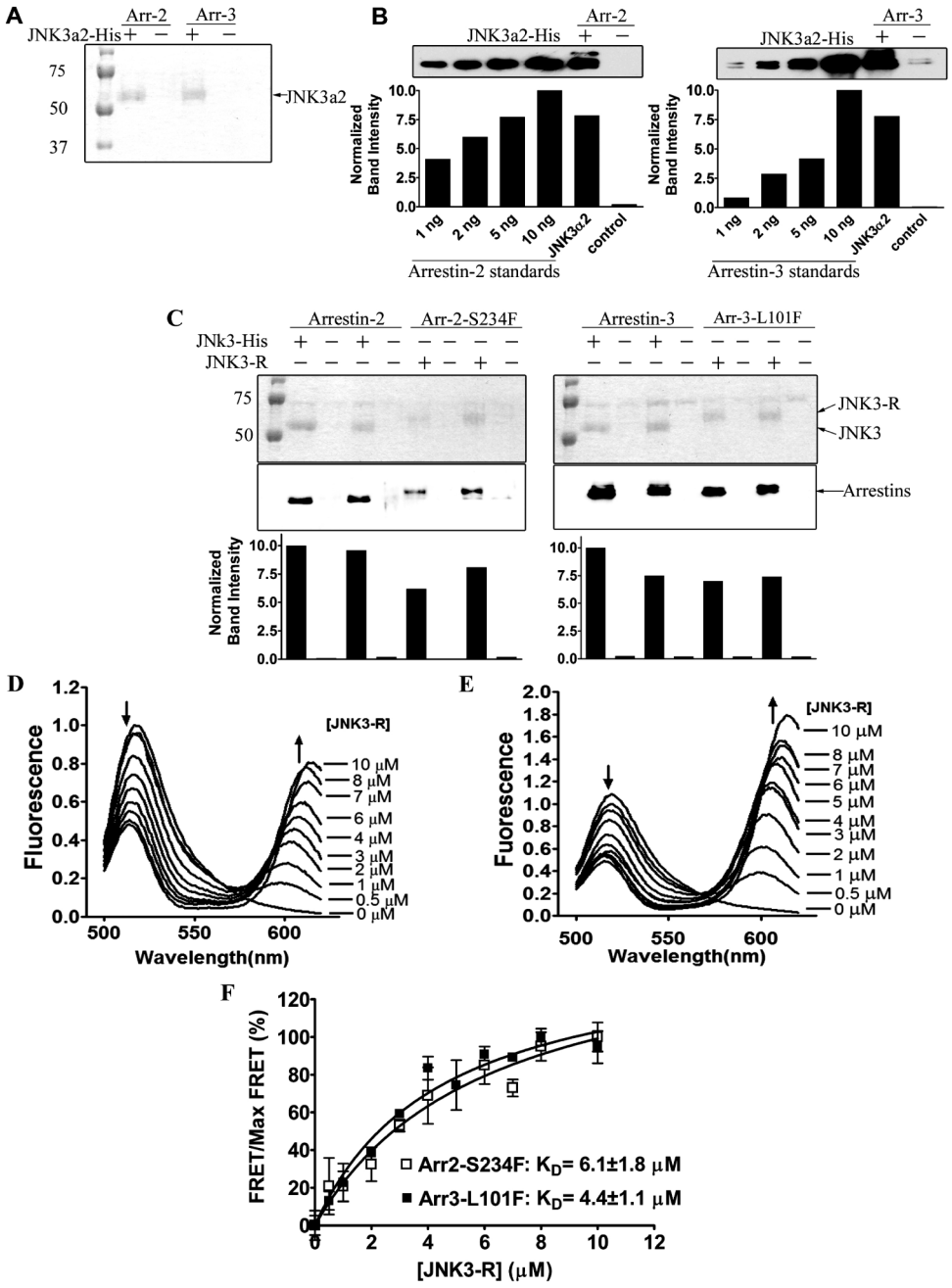

Fig. 2. Non-visual arrestins directly bind to JNK3α2 with comparable affinities

A. Coomassie staining of JNK3α2-His eluted from nickel-NTA column with imidazole, showing equal loading. **B.** Western blots of the eluates (1/5 loaded); lanes containing known amounts of purified arrestin-2 and -3 standards were used to generate calibration curves. Quantification shows that JNK3α2-His column retained 5.5 ± 0.9 and 7.7 ± 1.2 ng of arrestin-2 and –3, respectively (n=3). The results demonstrate direct interactions of both non-visual arrestins with JNK3α2-His. **C.** Fluorescent labeling does not appreciably affect arrestin interaction with JNK3α2. JNK3α2-His (JNK3-His) or Alexa-568-labeld JNK3α2-His (JNK3-R, which runs slightly slower on the gel) (20 mu;g) were loaded onto 50 mu;l nickel-NTA resin and incubated with purified WT arrestin-2, arrestin–3 or fluoresceine-

labeled arr-2-S234F or arr-3-L101F, as indicated. The columns were washed three times with binding buffer and specifically bound proteins were eluted. 1/5 of each elutate was analyzed by SDS-PAGE. Top panel: Coomassie staining of indicated eluted proteins. Middle panel: Western blot with pan-arrestin antibody. Bottom panel: quantification of the intensity of arrestin bands. The results of representative experiment out of three performed are shown. **D.** FRET between Arr-2-S234F (donor) and JNK3-R (acceptor). Representative emission spectra from experiments in which Arr3-L101F (50 nM) was incubated with indicated concentrations of JNK3-R (0–10 mu;M) with excitation at 485 nm. All spectra are normalized to donor-only fluorescence at 518 nm. **E.** FRET between Arr-3-L101F (donor) and JNK3-R (acceptor). Representative emission spectra from experiments in which Arr3-L101F (50 nM) was incubated with indicated concentrations of JNK3-R (0–10 mu;M) with excitation at 485 nm. All spectra are normalized to donor-only fluorescence at 518 nm. **F.** Binding affinity of non-visual arrestins for JNK3α2 were measured by FRET (panels **D, E**). Calculated apparent K_D of arrestin-2 and –3 binding to JNK3α2 were 6.1 ± 1.8 and 4.4 ± 1.1 μM, respectively (n=3).

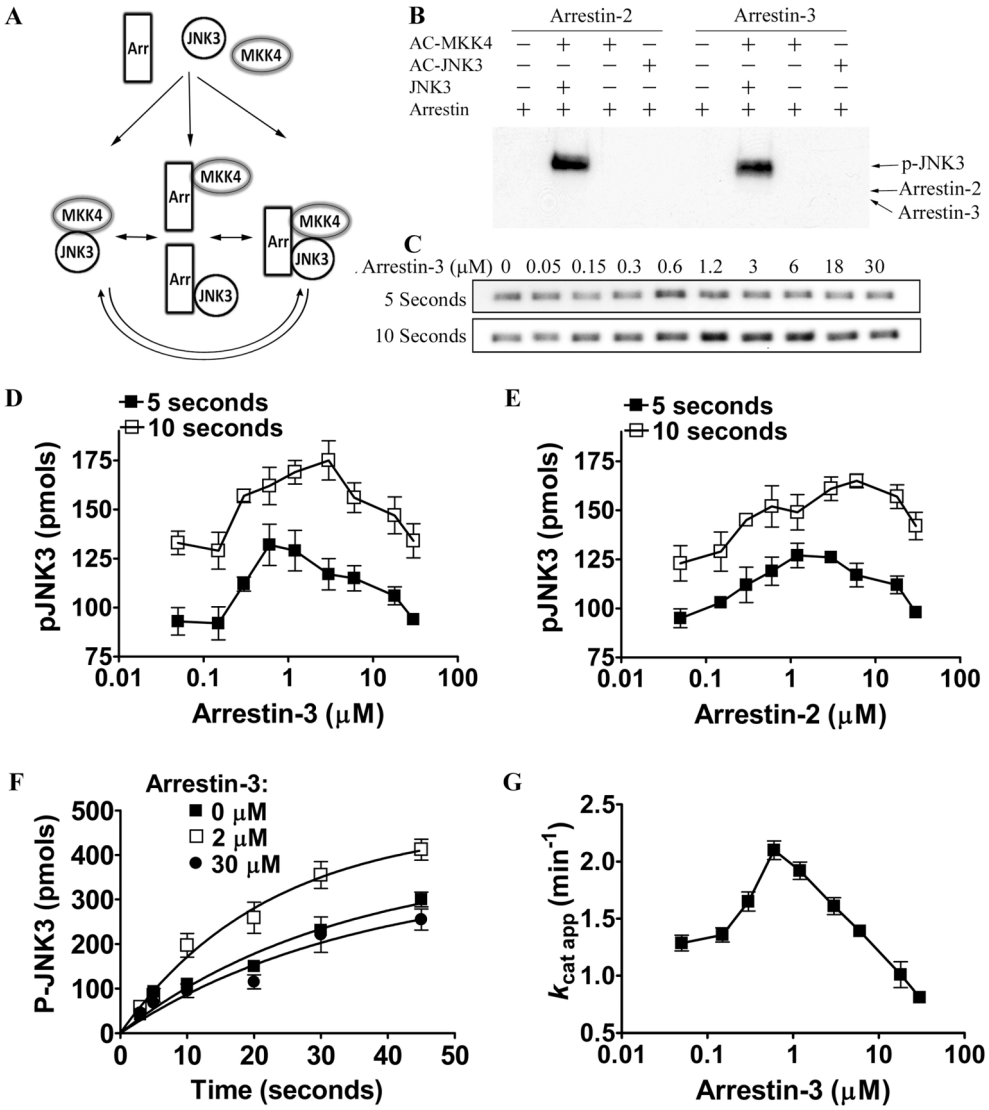

Figure 3. Biphasic effects of both non-visual arrestins on JNK3α2 activation by MKK4

A. A simplified three-state model showing scaffolding mechanism of the two-kinase signaling module. A, J and M stand for arrestin scaffold, JNK3α2, and upstream kinase MKK4, respectively. Kinases can exist in three states: a) interacting in solution; b) bound to scaffold to form incomplete complexes containing a single kinase; and c) simultaneously tethered by scaffold to form a complete two-kinase signaling complex. **B.** MKK4 and JNK3α2 do not phosphorylate arrestin-2 and -3. Indicated purified arrestins (2 mu;M) were incubated with active MKK4 (50 nM), active JNK3α2 (50 nM), or inactive JNK3α2 (0.5 mu;M), as indicated, in kinase buffer for 3 min. The reactions were stopped by 15 μl SDS sample buffer and the proteins were separated on 10% SDS-PAGE. The gel was dried and exposed to X-ray film. Autoradiogram from a representative experiment (out of three performed) is shown. **C.** Representative autoradiograms showing MKK4-phosphorylated JNK3α2 at indicated concentrations of arrestin-3 at 5 and 10 s. Solutions containing 50 nM active MKK4, 0.5 mu;M JNK3α2, and 0–30 mu;M arrestin-3 were premixed and incubated at 30°C for 15 mins. The reactions were initiated by the addition of 0.2 mM ATP (4 mu;Ci [γ-^{32}P]) and incubated at 30°C for indicated time. The reactions were stopped by the

addition of Laemmli SDS sample buffer, and subjected to PAGE on 10% gel. Autoradiogram from a representative experiment (out of three performed) is shown. **D, E.** JNK3α2 phosphorylation by MKK4 as a function of arrestin-3 (**D**) or arrestin-2 (**E**) concentration at indicated early time points (5 and 10 s). **F.** The time course of JNK3α2 phosphorylation by MKK4 at different arrestin concentrations (0, 2, and 30 mu;M). **G.** ATF2 phosphorylation by JNK3α2 activated by MKK4 at different arrestin-3 concentrations. Solutions containing 50 nM active MKK4, 1 mu;M JNK3α2, and 0–30 mu;M arrestin-3 were premixed and incubated at 30°C for 15 min. The reactions were initiated by the addition of 0.3 mM ATP and incubated at 30°C for 4 min. 7 ul of the reaction mixture were transferred to another reaction mixture containing 20 mu;M GST-ATF2 (1–115) and 0.3 mM radiolabelled [γ-^{32}P]-ATP (specific activity = 1×10^{15} cpm/mol) to final volume of 70 μl (1/10 dilution). Apparent JNK3α2 k_{cat} was determined plotted as a function of arrestin-3 concentration.